Applied Surface Science 528 (2020) 146955

Contents lists available at ScienceDirect

Applied Surface Science

journal homepage: www.elsevier.com/locate/apsusc

Full Length Article

Non-activated adsorption of methane on nickel surfaces induced by reduced work function

S. Raaen*, K.W.B. Hunvik

Physics Department, Norwegian University of Science and Technology (NTNU), N7491 Trondheim, Norway

ARTICLE INFO

Keywords:
Methane
Ni(100)
Muscovite mica
Ni nanoparticles
Adsorption

ABSTRACT

Adsorption of methane has been studied in ultrahigh vacuum environments on single crystalline *Ni*(100) as well as on *Ni* nano-particles on mica substrates. Experimental techniques have been X-ray and ultraviolet photoelectron spectroscopy (XPS and UPS) and temperature programmed desorption spectroscopy (TPD). In accordance with previous observations only physisorption of CH_4 is observed on pure nickel at temperatures below 130 K for exposures in the high vacuum regime. TPD in the temperature range from 200 to 300 K shows that chemisorption of methane takes place when the sample work function is lowered by about 0.7 eV by a surface treatment, which presumably exposes the surface to atomic hydrogen. The lowered work function enables charge transfer from the Ni conduction band to the methane affinity level which subsequent leads to dissociative chemisorption.

1. Introduction

Methane is in addition to being a greenhouse gas an important resource for the ammonia synthesis and for production of higher hydrocarbons [1–3]. A comprehensive understanding of surface reactions involving methane requires detailed studies of adsorption and desorption from various surfaces.

Absence of electric dipole or quadrupole moments and a high activation barrier for dissociative adsorption renders methane very non-reactive at metallic surfaces. Energy may be supplied to the gas by heating the sample [4–6]. The sticking coefficient of methane on various nickel surfaces is known to be extremely low and little adsorption is observed for exposures at pressures in the high vacuum regime [7–12]. The weak adsorption interactions have been modelled by density functional calculations [13,14]. Decomposition reactions of methane on nickel surfaces have been studied using pressures in the 1 Torr range [10], and activation energies have been obtained. Theoretical modelling of vibrational excited methane on nickel surfaces suggests that mode specific effects may be important for chemical reactivity [15]. Density functional calculations have shown that adsorbed *C* may be bonded with surface as well as subsurface atoms on stepped *Ni* surfaces upon exposure to CH_4 [16]. The methane sticking probability was found to be diminished by the presence of low coverage of *K* on *Ni*(100) and surfaces. This somewhat surprising finding was explained by an increased barrier for dissociation in the presence of *K*. Density functional calculations show that a dipole moment is induced in the transition state of the molecule and that the barrier for dissociation is given by the interaction between the induced dipole moment and the electrostatic field of the potassium atom [17]. Another study concluded that small amounts of sulfur on *Ni*(100) poison the methane dissociation reaction by a site blocking mechanism, which is consistent with a direct rather than a precursor mediated process [18]. Previous results suggest that the high pressure requirement can be bypassed in reactions where the dissociative adsorption of the reactant is activated by raising the kinetic energy of the impinging molecule [9,19].

The work function is a fundamental property of a metal surface, and work function changes are routinely used in the study of adsorption of atoms and molecules [20,21]. The present investigation concerns non-activated adsorption of methane on Ni surfaces in which the work function has been lowered by a surface modification prior to the adsorption of methane. The surface modification is argued to be caused by adsorption of atomic hydrogen. It is observed that desorption of methane occurs in the temperature region between 200 and 300*K* after non-activated exposure at low temperature.

2. Experimental

Temperature programmed desorption (TPD) spectra were obtained by using a shielded and differentially pumped Prisma quadrupole mass spectrometer (Pfeiffer). The mass spectrometer was positioned close to

* Corresponding author.
E-mail address: sraaen@ntnu.no (S. Raaen).

https://doi.org/10.1016/j.apsusc.2020.146955
Received 6 April 2020; Received in revised form 4 June 2020; Accepted 10 June 2020
Available online 16 June 2020

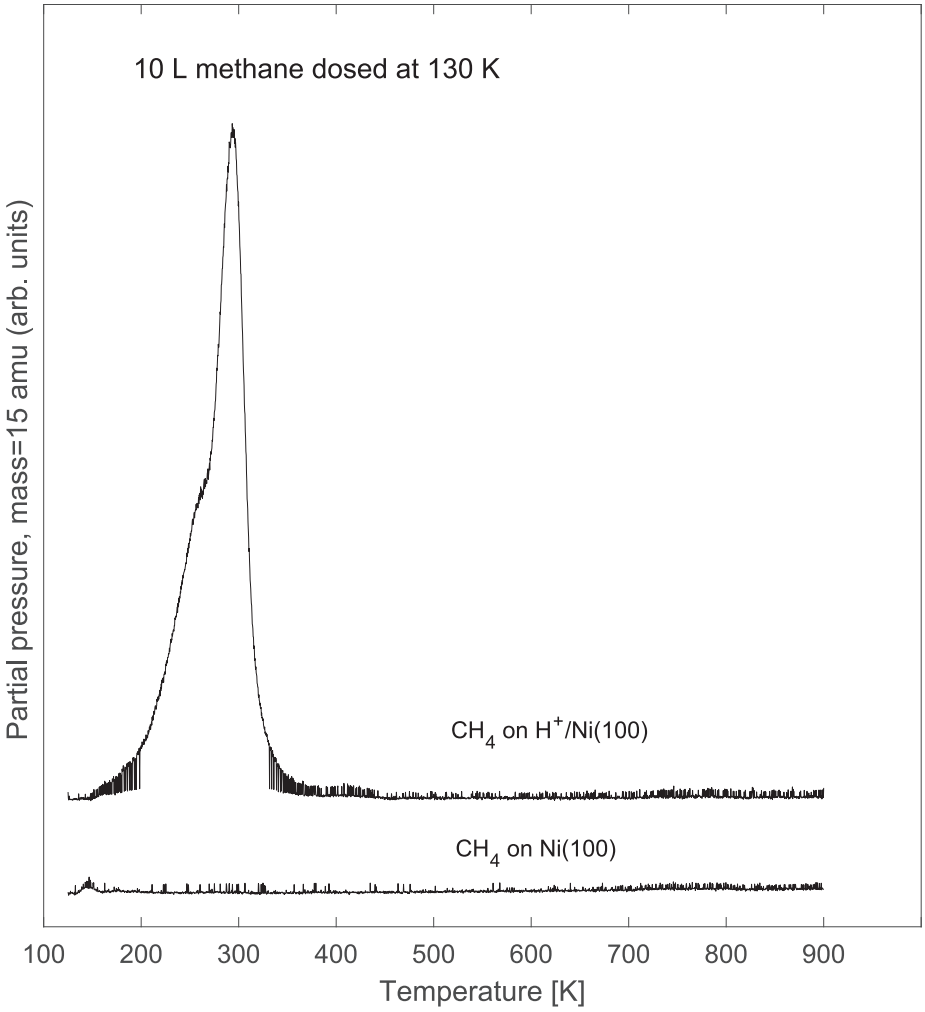

Fig. 1. TPD (mass = 15 amu) after exposure of 10 L methane to $Ni(100)$: Top spectrum is for hydrogen pre-treated sample, and bottom spectrum is for pure sample.

the sample surface during measurements to discriminate against spurious desorption from the sample support, and to obtain reproducible intensities that could be compared for different runs. Spectra were obtained from masses 2, 15, 18, 28, and 44 amu (atomic mass unit) simultaneously for all experimental runs. Mass 15 amu is a fragmentation product of methane which constitutes about 40% of the total mass spectrometer signal, and is recorded since there are no other significant fragmentation products at this mass. X-ray photoelectron spectrocopy (XPS) and ultra-violet photoelectron spectrocopy (UPS) measurements were recorded using a SES2002 spectrometer (Scienta) in conjunction with a monochromatized Al Kα X-ray source (Scienta) and a UVS300 He discharge lamp (Specs) which provided photons of energy $h\nu = 21.2$ eV. The sample work function was estimated by subtracting the width of the UPS from the photon energy using a sample bias of -5 V. The $Ni(100)$ crystal was cleaned by repeated Ar sputtering, flash heating and oxygen annealing. The quality of the Ni single crystal was verified by measuring a sharp FCC(100) low-energy electron diffraction (LEED) pattern. The fabrication of Ni nano-particles on muscovite mica substrates was made as previously reported [22]. A flood gun or a naked tungsten filament placed near the sample surface was used for charge neutralization during the photoemission measurements on the insulating samples. The tungsten filament was also used in the process of exposing the samples to atomic hydrogen, as discussed in the next chapter. Atomic force microscopy (AFM) measurements were performed in the peak force-tapping mode in air, using a ScanAsyst probe on a Nanoscope IV microscope (Digital Instruments). The AFM images were recorded at atmospheric conditions after the TPD runs had been completed.

3. Results and discussion

For the presented data, methane was dosed at a substrate temperature of 130 K. The dose of 10 L (Langmuir) was obtained by exposing at a pressure of $1{\cdot}10^{-7} Torr$ for a duration of 100 s, ($1L = 1{\cdot}10^{-6}$ s·Torr). The lower spectrum of Fig. 1 show TPD for exposure to pure $Ni(100)$. The spectrum is rather structureless, and the small feature near a temperature of 140 K show desorption of physisorbed CH_4. The upper spectrum of Fig. 1 show TPD for a similar methane dose on the same $Ni(100)$ sample which had been pre-treated as described below, presumably by exposure to atomic hydrogen. The CH_4 desorption spectrum which is observed in the temperature range between 200 and 300 K corresponds to chemisorption of methane. Kinetic

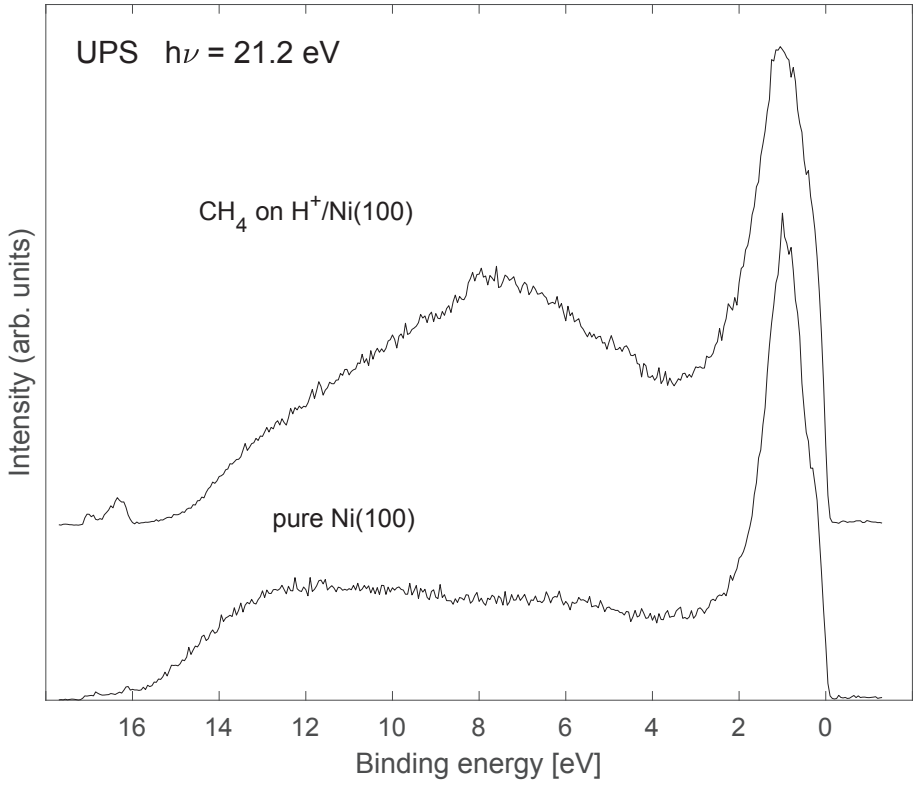

Fig. 2. UPS using the He-I line at $h\nu = 21.2eV$ of the valence band region of pure $Ni(100)$ (bottom spectrum) and $Ni(100)$ after exposure to $10L$ methane (top spectrum).

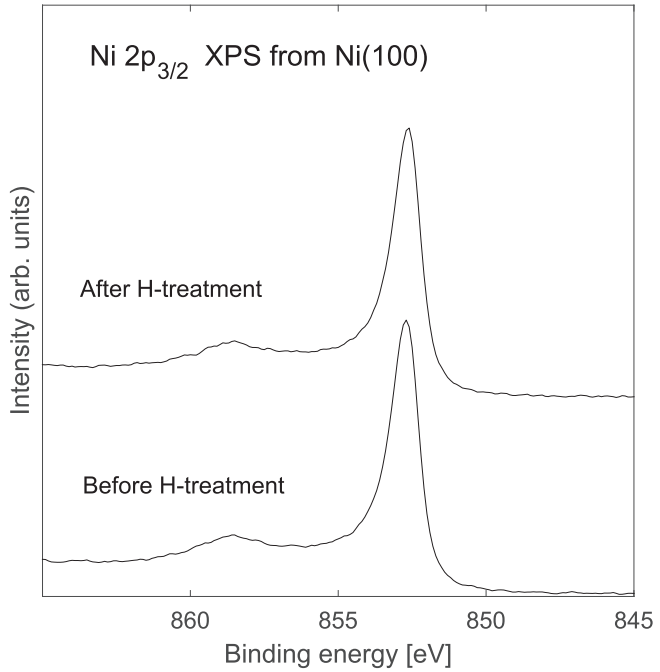

Fig. 3. Ni 2p XPS core levels of Ni(100) before and after hydrogen surface treatment. No significant changes are observed, which may support the assumption that the surface treatment is by atomic hydrogen.

parameters may be estimated for the initial desorption by fitting the low temperature edge of the TPD spectrum using the Polyani–Wigner equation. The kinetic parameters depend on the coverage and the assumption when extracting the parameters is that the coverage does not change more than a few percent for the region of the pre-edge that is being fitted [23,24,22]. For the top curve in Fig. 1 a desorption energy of about 0.15 eV is obtained. The vibrational prefactor is estimated to be about 8.0 s^{-1}.

The surface treatment of the *Ni* samples was performed by using the charge compensation filament in front of the sample as XPS spectra were recorded from the sample. The hydrogen atmosphere was from the background pressure in the chamber and was estimated to be about $5{\cdot}10^{-10}$Torr during the XPS measurements. The exposure time was about 40 min. This treatment had a surprising dramatic effect on the mass 15 amu TPD spectra, as seen in Fig. 1. Since hydrogen is not detected by XPS or UPS the main indication for atomic hydrogen on the surface is given by a reduction in sample work function of about 0.7 eV following the surface treatment. It is noted that a substantial change in work function typically takes place for a coverage of only a fraction of a monolayer. The work function of pure $Ni(100)$ was measured to be 5.27 eV. Contamination by oxygen or carbon monoxide typically increases the work function of a metal, by creating a surface dipole pointing inwards on the surface [25,26]. A dipole pointing outwards from the surface reduces the work function, and may be realized by adsorption of electropositive elements, e.g. alkali metals or rare earths, or hydrogen [27]. Fig. 2 show UPS spectra for clean $Ni(100)$ (bottom spectrum) and pre-treated $Ni(100)$ with a 10 L CH_4 exposure (top

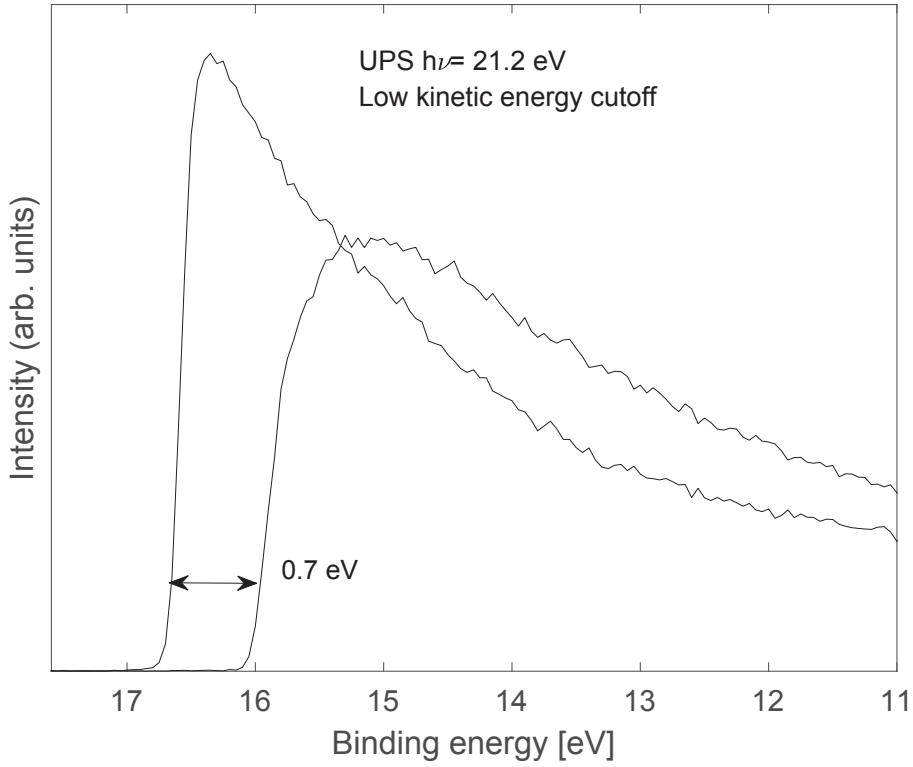

Fig. 4. The low kinetic energy cutoff in the UPS for pure *Ni*(100) (right cutoff) and hydrogen pre-treated *Ni*(100) (left cutoff). The sample was biased at a voltage of −5 V.

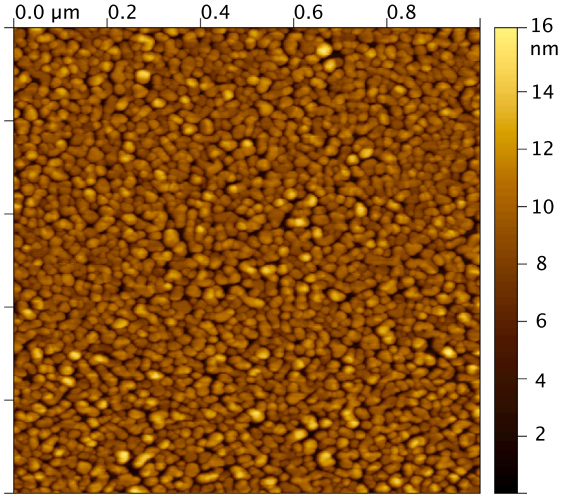

Fig. 5. AFM image of Ni nanoparticles on mica. The effective Ni coverage was 4 monolayers, and the sample was measured after annealing to 600 K and after removal from the vacuum system.

spectrum). Structures from 6 to 10*eV* binding energy in the upper spectrum may partly be due to a 6 eV Ni shake-up satellite [28] as well as adsorption of residual gases in the vacuum chamber, mainly carbon monoxide and water. In Fig. 3 are shown $Ni2p_{3/2}$ XPS before and after surface treatment. No significant changes are observed, which strengthen the interpretation of the surface treatment to be caused by H-adsorption, since hydrogen is the only element that is not detectable by photoelectron spectroscopy due to the very low photo-ionization cross-section. The Ni 2p correlation satellite is seen at a binding energy of 858 eV [28]. Measurements of the low kinetic energy cutoff in UPS, which show the work function change are shown in Fig. 4, for pure and pre-treated *Ni*(100).

The effect of enhanced methane adsorption for pre-treated Ni is not confined to the *Ni*(100) surface, and was initially observed for nanoparticles of Ni on muscovite mica substrates, since charge compensation is needed to perform photoemission experiments on these insulating samples [22,29]. The naked tungsten filament which was placed near the sample surface was used for charge compensation. Fig. 5 shows an AFM image of Ni which was deposited on the mica substrate and subsequently annealed to 600 K, and exhibits formation of Ni nano-particles. The effective Ni coverage in this image was 4 monolayers. In Fig. 6 are shown TPD results for an effective *Ni* coverage of 0.8 ML (monolayer). Desorption of methane from: Ni/mica (bottom curve), H-pre-treated Ni/mica (middle curve), and H-pre-treated Ni/mica and annealed to 600 K prior to the TPD experiment (top curve). Uncertainty in the intensity of the different spectra in the figure makes a directly comparison difficult. Methane was dosed at a temperature of 130 K using a dosage of 10 L. The difference between the two upper spectra in Fig. 6 are caused by a rearrangement of the Ni nano-structures as the sample is heated to 600 K. It has been reported that FCC metals has a tendency to form clusters of cubo-octahedral shape to minimize free energy [30,31]. For such clusters the number of terrace, step, and kink sites varies with the size of the cluster [32]. As the Ni/mica system is annealed the clusters will grow in size and the distribution of available adsorption sites may change to alter the desorption spectra [22].

The adsorption of methane on the pre-treated samples is argued to be related to the reduction of the work function. The electron affinity of

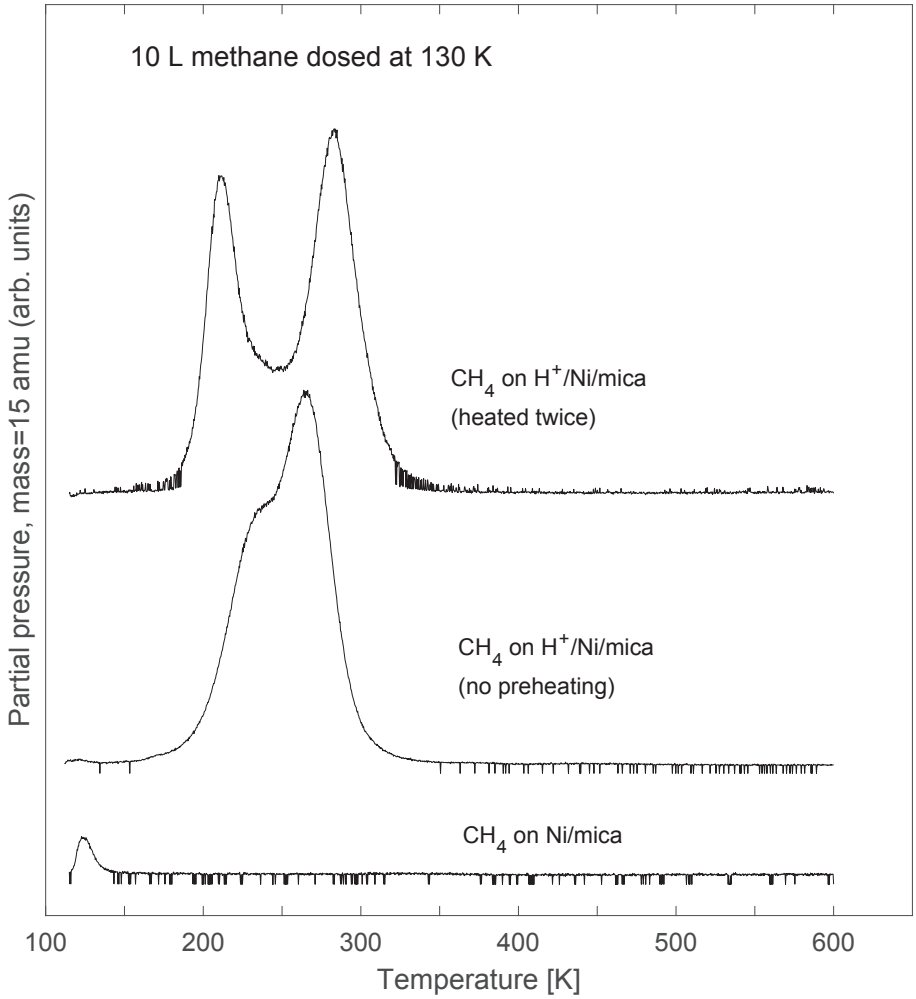

Fig. 6. TPD (mass = 15 amu) after exposure of 10 L methane to Ni/mica. Bottom curve: Pure Ni/mica. Middle curve: Hydrogen pre-treated Ni/mica (first temperature ramp). Top curve Hydrogen pre-treated Ni/mica (second temperature ramp).

methane has been estimated to be in the order of 1 eV [33,34]. A qualitative explanation is proposed with reference to the schematic energy level diagram which is shown in Fig. 7. The top diagram shows energy levels of separated metal and molecule. As the molecule approaches the metal surface electronic levels are lowered by the influence of the image potential of the surface [35]. In the case of hydrogen induced work function reduction (lower diagram) the affinity level of the molecule comes close enough to the metal Fermilevel to facilitate charge transfer, which is a crucial step for subsequent dissociative adsorption. Conceivably, the adsorption process results in CH_3 species on the surface. From the UPS in Fig. 2 it is evident that the *Ni*3*d* intensity at the Fermilevel stays largely unchanged following the work function reduction, thus retaining the reactivity and catalytic activity of nickel.

The details of the mechanisms leading to the work function reduction is not completely understood. Adsorption of CH_4 is not observed when the charge neutralization is done by using a low energy flood gun. This was tested on both the Ni crystal as well as the Ni/mica nanoparticle system. Also, no adsorption of CH_4 was found when the hot filament was used without using the X-ray source. This indicates that the hot filament in conjunction with Al $K\alpha$ X-rays is required to deposit hydrogen on the Ni-surface in these experiments. It is noted that the only indication of hydrogen on the surface is the reduction in the sample work function and the observation that no other unexpected elements are observed in XPS from the samples. It should also be noted that exposure to H_2, CO, H_2O, or CO_2 prior to methane exposure had no significant effect on the adsorption of methane.

4. Conclusions

Non-activated adsorption of methane was observed at pressures in the high-vacuum regime for *Ni* samples that had been pre-treated by using a hot tungsten filament during XPS measurements. It is argued that the ambient hydrogen pressure of about $5{\cdot}10^{-10}$Torr during this process was sufficient to expose the surface to atomic hydrogen, which in turn resulted in a reduction in work function which facilitated charge transfer to the methane affinity level and dissociative adsorption on the *Ni* samples.

These findings may have relevance to adsorption processes in reactions that involves methane at high temperature and pressure, in that radicals that alter the work function of nano-particles may be present.

Further work is needed to unravel the details of the surface treatment that lowers the sample work function on Ni substrates.

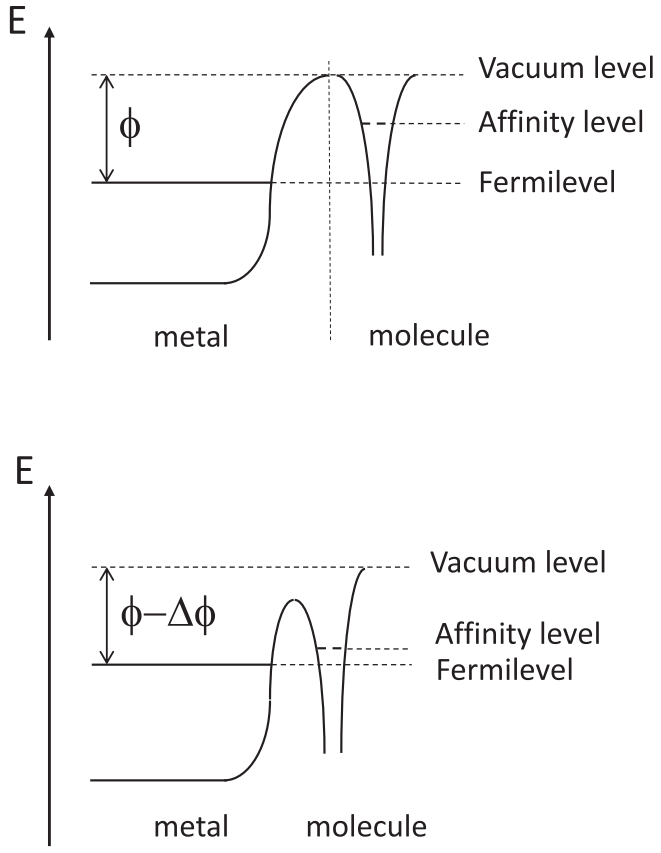

Fig. 7. Schematic energy level diagram as a molecule approaches a metal surface. On top is shown energy levels for separate metal and molecule, and on bottom is shown energy levels as the molecule approaches the metal surface. The affinity level of the molecule comes close enough to the Fermilevel to facilitate charge transfer from the metal. Φ is the work function and ΔΦ is the reduction in the work function following the hydrogen treatment.

Acknowledgments

We are grateful to Anna Støvneng for her contributions to the AFM measurements. This work was supported by the Research Council of Norway (RCN) under project No. NFR 250728.

References

[1] G.F. Froment, Production of synthesis gas by steam- and co2-reforming of natural gas, J. Mol. Catal. A 163 (2000) 147–156, https://doi.org/10.1016/S1381-1169(00)00407-6.
[2] R.G. Bergman, Activation of alkanes with organotransition metal complexes, Science 223 (1984) 902–908, https://doi.org/10.1126/science.223.4639.902.
[3] T. Fuhrmann, M. Kinne, B. Tränkenschuh, C. Papp, J. Zhu, R. Denecke, H.-P. Steinrück, Activated adsorption of methane on pt(1 1 1) — an in situ xps study, New J. Phys. 7 (2005) 107, https://doi.org/10.1088/1367-2630/7/1/107.
[4] H.F. Winters, The activated, dissociative chemisorption of methane on tungsten, J. Chem. Phys. 62 (1975) 2454–2460, https://doi.org/10.1063/1.430722.
[5] J.T. Yates Jr., T.E. Madey, The adsorption of methane by tungsten (100), Surf. Sci. 28 (1971) 437–459, https://doi.org/10.1016/0039-6028(71)90054-9.
[6] T.E. Madey, Adsorption and displacement processes on w(111) involving ch4, h2, and o2, Surf. Sci. 29 (1972) 571–589, https://doi.org/10.1016/0039-6028(72)90238-5.
[7] F.C. Schouten, E. Kaleveld, G. Bootsma, Aes-leed-ellipsometry study of the kinetics of the interaction of methane with ni(110), Surf. Sci. 63 (1977) 460–474, https://doi.org/10.1016/0039-6028(77)90359-4.
[8] F.C. Schouten, O.L.J. Guzeman, G. Bootsma, Interaction of methane with ni(111) and ni(1oo); diffusion of carbon into nickel through the (100) surface; an aes-leed study, Surf. Sci. 87 (1979) 1–12, https://doi.org/10.1016/0039-6028(79)90164-X.
[9] M.B. Lee, Q.Y. Yang, S.L. Tang, S.T. Ceyer, Activated dissociative chemisorption of ch4 on ni(111): Observation of a mehyl radical and implication for the pressure gap in catalysis, J. Chem. Phys. 85 (1986) 1693, https://doi.org/10.1063/1.451211 1692.
[10] T.P. Beebe, D.W. Goodman, B.D. Kay, J.T. Yates, Kinetics of the activated dissociative adsorption of methane on the low index planes of nickel single crystal surfaces, J. Chem. Phys. 87 (1987) 2305–2315, https://doi.org/10.1063/1.453162.
[11] I. Chorkendorff, I. Alstrup, S. Ullmann, Xps study of chemisorption of ch4 on ni (100), Surf. Sci. 227 (1990) 291–296, https://doi.org/10.1016/S0039-6028(05)80017-2.
[12] P.M. Holmblad, J. Wambach, I. Chorkendorff, Molecular beam study of dissociative sticking of methane on ni(100), J. Chem. Phys. 102 (1995) 8255, https://doi.org/10.1063/1.468955.
[13] S. González, F. Viñes, J.F. García, Y. Erazoa, F. Illas, A df-vdwstudy of the ch4 adsorption on different ni surfaces, Surface Sci. 625 (2014) 64–68, https://doi.org/10.1016/j.susc.2014.03.012.
[14] M. Haroun, P. Moussounda, P. Légaré, Dissociative adsorption of methane on ni (111) surface with and without adatom: A theoretical study, J. Molecular Structure: THEOCHEM 903 (2009) 83–88, https://doi.org/10.1016/j.theochem.2008.10.049.
[15] L. Halonen, S.L. Bernasek, D.J. Nesbitt, Reactivity of vibrationally excited methane on nickel surfaces, J. Chem. Phys. 115 (2001) 5611–5619, https://doi.org/10.1063/1.1398075.
[16] R.L. Arevalo, S.M. Aspera, M.C.S. Escaño, H. Nakanishi, H. Kasai, Tuning methane decomposition on stepped ni surface: the role of subsurface atoms in catalyst design, Sci. Rep. 7 (2017) 13963, https://doi.org/10.1038/s41598-017-14050-3.
[17] H.S. Bengaard, I. Alstrup, I. Chorkendorff, S. Ullmann, J.R. Rostrup-Nielsen, J.K. Nørskov, Chemisorption of methane on ni(100) and ni(111) surfaces with preadsorbed potassium, J. Catal. 187 (1999) 238–244, https://doi.org/10.1006/jcat.1999.2612.
[18] X. Jiang, D.W. Goodman, The effect of sulfur on the dissociative adsorption of methane on nickel, Cat. Lett. 4 (1990) 173–180, https://doi.org/10.1007/BF00765701.
[19] S. Nave, A.K. Tiwari, B. Jackson, Methane dissociation and adsorption on ni(111), pt(111), ni(100), pt(100), and pt(110)-(1x2):energetic study, J. Chem. Phys. 132 (2010), https://doi.org/10.1063/1.3297885 054705.
[20] A. Michaelides, P. Hu, M.-H. Lee, A. Alavi, D.A. King, Resolution of an ancient surface science anomaly: Work function change induced by n adsorption on w(100), Phys. Rev. Lett. 90 (2003), https://doi.org/10.1103/PhysRevLett.90.246103 246103.
[21] P.S. Bagus, V. Staemmler, C. Wöll, Exchangelike effects for closed-shell adsorbates: Interface dipole and work function, Phys. Rev. Lett. 89 (2002), https://doi.org/10.1103/PhysRevLett.89.096104 096104.
[22] K.W.B. Hunvik, A. Støvneng, B. Pacáková, S. Raaen, Co desorption from nickel-decorated muscovite mica, App. Surf. Sci. 490 (2019) 430–435, https://doi.org/10.1016/j.apsusc.2019.06.073.
[23] D.A. King, Thermal desorption from metal surfaces: A review, Surf. Sci. 47 (1975) 384–402, https://doi.org/10.1016/0039-6028(75)90302-7.
[24] J.B. Miller, H.R. Siddiqui, S.M. Gates, J.N. Russell Jr, J.T. Yates Jr, J.C. Tully, M.J. Cardillo, Extraction of kinetic parameters in temperature programmed desorption: A comparison of methods, J. Chem. Phys. 87 (1987) 6725–6732, https://doi.org/10.1063/1.453409.
[25] J. Bardeen, Theory of the work function. ii. the surface double layer, Phys. Rev. 49 (1936) 653, https://doi.org/10.1103/PhysRev.49.653.
[26] T.N. Taylor, P.J. Estrup, Carbon monoxide adsorption on ni(110), J. Vac. Sci. Technol. 10 (1973) 26–30, https://doi.org/10.1116/1.1317970.
[27] J.C.P. Mignolet, Studies in contact potentials. part i. —the adsorption of some gases on evaporated nickel films, Discuss. Faraday Soc. 8 (1950) 105–114, https://doi.org/10.1039/DF9500800105.
[28] G.K. Wertheim, S. Hüfner, Systematics in core level asymmetries in xps spectra of ni, Phys. Lett. A 51 (1975) 301–303, https://doi.org/10.1016/0375-9601(75)90458-2.
[29] K.W.B. Hunvik, B. Pacáková, S. Raaen, Co_2 adsorption on pure and oxidized ni nano-structures on muscovite mica, unpublished.
[30] R.A. van Santen, M. Neurock, Molecular Heterogeneous Catalysis, Wiley-VCH, 2006.
[31] G.C. Bond, Small particles of the platinum metals, Platinum Met. Rev. 19 (4) (1975) 126–134.
[32] C.A. de Araujo Filho, D.Y. Murzin, A structure sensitivity approach to temperature programmed desorption, Appl. Catalysis A, General 550 (2018) 48–56, https://doi.org/10.1016/j.apcata.2017.11.001.
[33] A. Ramírez-Solís, On the accuracy of the complete basis set extrapolation for anionic systems: a case study of the electron affinity of methane, Comput. Chem. 2 (2014) 31–41, https://doi.org/10.4236/cc.2014.22005.
[34] CRC Handbook of Chemistry and Physics, vol. 47, CRC Press, Boca Raton, 1986-1987.
[35] P.M. Echenique, J.B. Pendry, The existence and detection of rydberg states at surfaces, J. Phys. C: Solid State Phys. 11 (1978) 2065–2075, https://doi.org/10.1088/0022-3719/11/10/017.